

Multi-Class ensemble classification framework with multi-layered feature extraction and ranking for Diabetic retinopathy data

Deepthi Kalwa¹, M.S. Josephine², V. JeyabalaRaja³

¹Department of CSE, Dr. MGR Educational & Research Institute, Chennai 600095, India

²Department of Computer Applications, Dr. MGR Educational & Research Institute, Chennai 600095, India

³Department of CSE, Velammal Engineering College, Chennai 600066, India

Abstract

Diabetic retinopathy (DR) remains one of the most prevalent causes of vision loss among adults, especially those with long-standing diabetes. It manifests through progressive damage to the small blood vessels in the retina, resulting in visible lesions like microaneurysms, hemorrhages, and both soft and hard exudates. Fundus imaging, a non-invasive diagnostic method, has become essential in identifying these retinal abnormalities. Recent improvements in image contrast techniques have enhanced the visualization of subtle lesions, enabling more precise and earlier detection of DR. By highlighting the morphological differences in the retinal structure, contrast-enhanced fundus images serve as a robust foundation for automated diagnostic systems and clinical evaluations, ultimately aiding in the timely management of DR to prevent irreversible blindness. Diabetic Retinopathy (DR) is a microvascular complication arising from prolonged diabetes, primarily affecting the retinal blood vessels. The probability of developing DR increases significantly with the patient's age and the number of years since being diagnosed with diabetes. Elevated and poorly managed blood glucose levels, along with erratic fluctuations in blood pressure, contribute to vascular damage, making the eyes more susceptible to retinopathy. The interplay between these physiological factors leads to the progressive degeneration of retinal capillaries, emphasizing the importance of long-term metabolic control in preventing or delaying the onset of DR. Early detection and classification of Diabetic Retinopathy (DR) are crucial in preventing irreversible vision loss. DR progresses through distinct stages, ranging from mild non-proliferative signs to advanced proliferative forms, each requiring specific clinical interventions. Manual diagnosis using retinal fundus images is not only time-consuming and labor-intensive but also depends on the availability of trained ophthalmologists. The inherent subjectivity in human assessment and the growing number of diabetic patients make manual screening an unsustainable solution. Therefore, automated systems based on image classification offer a promising alternative for timely and accurate identification of DR stages, enabling scalable and efficient screening protocols in clinical practice. Diagnosing Diabetic Retinopathy (DR) is often hindered by irregularities in contrast and brightness in fundus images, which obscure the detection of lesions. This study introduces a novel technique involving multi-level threshold-based filtering combined with an ensemble feature extraction framework. Four distinct sets of image features are utilized to accurately segment the retinal regions. A region-growing method, refined through threshold optimization, eliminates over-segmented and noisy areas, thereby enhancing the reliability of feature selection. These refined features are then fed into an ensemble classification model to improve diagnostic accuracy. Experimental validation on diverse DR datasets confirms that this method surpasses traditional techniques in precision and robustness, offering a more dependable solution for early DR detection.

Keywords: diabetic retinopathy, probabilistic segmentation, support vector machine, ensemble learning model

How to cite this article: Kalwa D, Josephine MS, JeyabalaRaja V. Multi-Class ensemble classification framework with multi-layered feature extraction and ranking for Diabetic retinopathy data. *Int J Drug Deliv Technol.* 2026;16(55s): 739-752. DOI: 10.25258/ijddt.16.55s.74

Source of support: Nil.

Conflict of interest: None.

1. Introduction

Due to the variability of background noise and dynamic variation of retinopathies, the recognition of DR has become more challenging. Diabetic retinopathy (DR) is a type of specific eye disease associated with diabetes caused by long-term high blood glucose levels, mainly damage to the eyes by suggestive name. DR is a disease that often occurs after diabetes. Early detection and treatment of DR

in diabetic patients is very important. If not treated early, it can develop more serious complications for patients. Diabetic retinopathy is a disease caused by damage to blood vessels in the retina. If the disease progresses, it may eventually lead to blindness. Diabetes is currently the fifth global cause of blindness. Diabetic retinopathy is the main cause of vision loss worldwide. In 2020, there were approximately 500 million diabetic eye diseases worldwide. By 2025, It will be increase to 800

million. In the diagnosis of this condition, feature extraction is very important. If there is diabetes, it is worth considering whether there is retinopathy. Among patients, the manifestations of retinopathy are different, including different angles, forms, textures and intensities. Due to the variability of DR manifestations, it is very difficult to extract the key feature in large-volume retinal data. The main purpose of feature extraction is to provide an analytical and robust feature identification method. Diabetic retinopathy (DR) is a specific eye disease related to diabetes due to damage to blood vessels of the retina for a long time, mainly diabetic retinopathy. However, the lack of available data worsens the current issue of diabetic retinopathy, as delays in medical diagnosis are common [3-5]. The high prevalence of this condition can be attributed to inadequate care and attention provided by healthcare professionals. It is concerning that almost half of all diabetes patients who have experienced diabetic retinopathy have not received sufficient medical attention. Individuals who have had diabetes for more than ten years are especially at risk of developing retinopathy. Based on my professional expertise, I firmly believe that the duration of diabetes is the most reliable indicator of the likelihood of developing this condition. The progression of diabetic retinopathy is widely acknowledged as a significant eye disease. Based on available evidence, timely medical intervention is crucial. It is crucial to effectively manage and prevent the advancement of this condition [6]. The World Health Organization (WHO) emphasizes that diabetic retinopathy is an urgent matter that requires immediate attention from governmental bodies and medical professionals. It is estimated that approximately 18% of individuals with diabetes are affected by this condition. Diabetic retinopathy is a condition that can significantly impact a patient's eyesight. It primarily affects the blood vessels of the retina, which is a light-sensitive tissue located at the back of the eye. As a result of this condition, the eye becomes more vulnerable to damage. To diagnose diabetic retinopathy, a comprehensive dilated eye examination called fluorescein angiography is typically performed. This procedure requires the expertise of ophthalmologists and other medical professionals. However, due to its time-consuming nature and dependence on the skill of practitioners, ongoing research is being conducted to discover more efficient alternatives. Therefore, it is crucial for medical professionals to be vigilant and consider this condition as a potential cause for any visual impairments or abnormalities observed in patients. Diabetic retinopathy can have mild vision problems as its first manifestation or be completely asymptomatic at the onset, but if not diagnosed and treated, it can progress further to severe visual impairment. One of the most notable characteristics of DR is the generation of abnormal blood vessels.

These microangiopathies were reported on retinopathy, both in the body of the retina and in the iris. Increased capillary permeability and capillary closure were detected concurrently with retina thickening. DR is associated with the appearance of the new blood vessels on the iris or retina. NPDR is the less severe form of the disease while PDR is the more severe manifestation marked by new veins on the eye. The retina itself normally does not manifest symptoms, and it's necessary to evaluate at the early stages to guarantee timely intervention. If DR is not diagnosed and treated properly, it can cause extensive negative consequences to the patient. In order to help recall previous experience and identify these characteristic features, this condition can be enrolled into the manual classification as normal, mild, moderate, or severe. A ratio between people who fall in each class in the given database is not 1:1 due to this typical artifact called class imbalance. For example, if we use medical diagnosis data, the ratio between people who are really ill and people who are not can be much different. If the prevalence of the disease is low, existing model can easily omit the class that has smaller count, and a model can perform badly. This is an adverse effect called overlook problem, which was proved by Bradley's landmark studies. Biased training data due to different data distribution between majority class and minority class, was called the bias problem. Three kinds of common proposals to deal with imbalanced DR datasets: oversampling the minority class, undersampling the majority class, and cost-sensitive learning. It is a well-known phenomenon that they all have common disadvantages because most of the methods easily introduce information loss or they can cause overfitting, or they demand more time and internal memory for the cost-sensitive learning. Covariate shift occurs when the distribution of the input feature is different between the classes. This could happen when information is gathered from multiple sources or at different times and the data is not identical in all input dimension [9]. This makes it difficult to infer the distribution of the class and predict the class label accurately. A class imbalance in the DR datasets would affect the accuracy, bias outputs and overfit the algorithms used for the machine learning. The existing modelling approach often fails to address the minority class as these models yield a suboptimal performance. Further, the use of multiple machine learning models for a joint inference, known as ensemble learning, can be used to correct model underperformance. Although computation-intensive, it has been implemented successfully in practice [11]. Class imbalance can also be addressed using deep learning or transfer learning that have been put forward recently as alternate methods for DR datasets. These include random oversampling, synthetic or feature augmentation oversampling and adaptive synthetic oversampling [11]. As we know,

resampling includes oversampling, undersampling and so on. There are some reasons to believe that oversampling and undersampling are much stronger for both binary or multiclass imbalanced classification types of DR. These class essentially-independent techniques outperform all other techniques or importantly, the combination of preprocessing and learning. From the literature, it is quite evident that preprocessing is helpful for balancing the distribution of variables first. Random oversampling randomly replicates the instances of the minority class until balanced class distribution is achieved. Obviously, this is a simplest technique in which some instances are elided because of being the same as existing ones. Since the elision process is performed randomly, we may face the overfitting problem. It also increases computation time. Synthetic oversampling is developed based on synthetic or fake instances that are generated in bootstrapping and bagging techniques [12]. Moreover, because the analysis of the DR tissue is crucial for diagnosis and treatment in patients, more accurate DR segmentation is important in the automatic diagnosis phase.

2. Related works

The perfect segmented DR area can be attained through the advanced capabilities of a neural network. This method requires the use of varied thresholds for different image regions, resulting in a substantial improvement in segmentation accuracy. Nevertheless, a neural network-based approach is used in this study to analyze and interpret these complex images expertly. This methodology results in a dependable tool for identifying DR lesions, ensuring accurate diagnosis. This is one of the methodology, which consists of a multistep approach for unusually identifying the lesion. This paper provides one of the first solutions that make use of automated image processing as well as extensive mathematical, computer science and statistical knowledge for the detection and diagnosis of lesions that are of complex morphology. In addition, the statistical shape model (SSM), which combines shape matching, representation, and search principles, is also used to segment the data using the (set) method. Finally, in order to achieve highest level of accuracy of diagnosis, principal component analysis (PCA) is used to make the precise delineation of the lesions in order to improve patient management. This could be one of the strategies that has the potential to revolutionize radiology. Therefore, this research has the potential to generate a positive impact. [11] utilized image preprocessing methods, including Gaussian algorithms and mean filter smoothing, to capture DR images. The image was partitioned into distinct areas based on important image features to eliminate staircase edges and enhance image quality. Nevertheless, DR segmentation in medical imaging may be complex due to the DR similarity to other

organs and changes in image contrast and intensity, leading to errors. Nonetheless, technological advancements have improved the precision of medical imaging. The algorithm's unpredictability feature prevents it from being stuck in a suboptimal solution, potentially revolutionizing how medical professionals approach slice-to-volume registration. To avoid uncertainty and prevent being stuck in local minima, a clever application of rigid-body transformation was used for the registration process. Trilinear interpolation is a frequently used precise method in medical imaging. The usefulness of image slicing from various perspectives is limited. To solve the problem of uneven content in images, a new non-linear cerebral registration method was presented by [12]. The study showed that combining different techniques, including non-linear registration, cortical surface extraction, tissue classification, linear registration, and resampling into a stereotaxic space, can greatly improve the cortical registration process. The significance of the linear aspect of the transformation was emphasized as a crucial factor in the registration process. An improved model has been developed to effectively tackle all the aforementioned challenges and enhance overall performance. The implementation of deep learning techniques effectively resolves these issues. Deep learning has demonstrated significant advancements in a range of natural language comprehension tasks, including subject classification, medical image analysis, and sentiment analysis[13]. The key components of deep learning include convolutional neural networks, recurrent neural networks, and other advanced algorithms, all of which contribute to its efficacy. Moreover, technical deep learning does use mostly some techniques mentioned above like neural networks, deep belief networks and autoencoders which are fundamentally important in order for it to success. Some of the most important and fundamental technique in using physiological features for deep learning is the use of convolutional neural network to represent deep learning features and improve their ability. In Convolutional Neural Networks (ConvNets), neurons in interior layers take as an input. Each neuron performs a weighted sum of all the received input and add it in an activation function like "relu", "sigmoid", "softmax" to produce an output. In order to achieve better performance, CNN network optimizes their loss function, optimizer, learning rate and decay rate. One of the advantages of using this type of techniques is that it catalyze using deep learning in better and more efficiently way. In addition, Convolutional Neural Networks (CNNs) require significantly less pre-processing compared to other deep learning or machine learning techniques. The neural network component is primarily used for feature extraction, especially in the field of image processing. Within the convolution layer, filters are used to traverse the input image. These filters

multiply the pixel values of the image by their corresponding filter values, resulting in a convolution matrix[14]. The intent of this conversation is to detect and classify lesions (in particular, those associated with DR), as they appear in fundus images.[14]An algorithm to perform this task has been created by Anderson Rocha et al. This is an end-to-end algorithm with an efficient approach to analyze the fundus images in a precise way. The method can accurately detect both white lesion and red lesion lesion without the need of any pre- or post-processing methods. The effectiveness of this algorithm is going to be assessed. In a study conducted by Keith A. researchers use 5-fold cross-validation on a dataset containing 687 images of normal retina, 245 images containing bright lesions and 191 images containing broken blood vessels to identify red lesions and detect white lesions on test data consisting of 109 images that acquired from reports assuring the existence of both bright lesions and red lesions on their test data.[15]The study determined the algorithm was effective with an AUC of 95.3%. With this visual dictionary in cross-dataset analysis for general lesions has sites accuracy rates of 93.3% for red lesions. These results presented evidence that training with images acquired across various images settings. Red lesions have size factors and appear as red patches of the fundus, resulting in their success with this approach. Proliferative diabetic retinopathy, thought a relatively less common condition to diabetic retinopathy, carries the greatest risk of blindness caused by the disease. The second operation of the algorithm involves a local/relative detection of lesion zones. The initialization of the system starts by processing the input retinal images through detecting the background from the regions of noise. The next step for the accuracy of the detection of the system was to implement these methods. The optic disc contour can also be detected through proper techniques. To achieve these processes of finding the optic disc, blood vessels were first segmented after an average filter and thresholding methods were applied. Then a combined technique of hybrid fuzzy method is implemented to detect both the dark and bright lesions[16]. The use of block diagram and digital retinal imaging technologies in this field cannot be over emphasised. The recent advancement by Hsu W has made it an important component of eye screening programs worldwide, due to its high accuracy and reproducibility in the diagnosis and staging of diabetic retinopathy (DR)[17]. Automated red lesion detection can significantly reduce the workload of these screenings, allowing health practitioners to become more efficient and thus more effectively cater for diabetic patients by far reducing the reliance of the manual interpretation of images [20]. A degenerative disease of the eye requires the development of a well suited method to clearly and accurately detect the classification of mild and

severe stages of the condition. Evidence shows that automated detection techniques which identify vascular anomalies in images of diabetic retinopathy using a scale and orientation-selective Gabor filter, known as banks, have shown to be very effective in detecting these lesions in the retinal images. Proposed diagnosis strategy that uses Gabor filter to image analysis and categorises cases as either mild or severe cases of Diabetic macular edema (DME), a condition that requires high sensitivity and accuracy for detection. The background colour should be able to identify the exudates, vital in the diagnostic process. Acceptable results can be obtained if this technique is combined with computer support for morphological reconstruction, to mark out the exudates by their structural characteristics. It was important to be able to detect the location of the optic disc, which can be achieved [21]. They used a detection rule based on binary-hypothesis testing and simplifying it into a series of yes/no questions. The paper discusses adjustment and thresholding methods as well as their utilisation. To figure out whether each candidate pixel is indeed an exudate, more than 50 descriptors are extracted. The informational content of these descriptors is well investigated to select the most relevant ones[22]. Preprocessing of the images include uniform lighting, adjustment of image intensities, contrast and morphological operations. A new detection method is developed to distinguish DR and to train its development A Linear Support Vector Machine (SVM) gives promising results for DR accurate detection. Precise Non-Proliferative Diabetes Retinopathy detection is achieved with DR detection sensitivity of 96% and DR specificity of 92%. Model introduced two different strategies to monitor the progress of the diabetic retinopathy (DR) by counting microaneurysms. This binocular model was useful for the detection of different diseases. Although the model initially has low difficulties, the challenges occur when the training and testing the models with the dataset that has insufficient amount of data. For those challenges, more studies have to be conducted. In a study conducted [23-24], the specific model was designed to detect the red lesions that exist in the paired retinal images. In their study conducted by [25], the retinal images were classified with the features that obtained by the algorithms that implement anatomical parts and lesions detection. The performance of this method was measured. In this study, the researchers perform a comparison with KELM method and explained that if the classifier work with the specific dataset, the bagging technique can increase the classifier performance. In a study conducted [26], a hybrid classifier was introduced in their study, with an active learning technique. The training with 80% of annotated retinal images from the MESSIDOR dataset was done. The resulted model achieved approximately

82% of accuracy rate with the categorizing images among the different groups. Because the diabetic retinopathy is a most common cause of blindness, the exudates are widely occurring diseases around the world. It is important to detect the exudates, to prevent the complications that may happen. The researchers used the fuzzy c-means and the median filter technique to enhance the findings. These techniques separated every feature from the classes, and it is removed the noisy parts. [27] introduced a method that uses the Histograms for image processing. Early detection of diseases without professional help is always important. With the conditions such as glaucoma, diabetic retinopathy, or macular degeneration, it may cause blindness if not detected and diagnosed on time. Therefore, retinal objects such as retinal vessels identification and their diagnosis are crucial. Retinal vessels anomalies can cause poor and uneven blood flow to the retina, and it might be harmful. Research improved the knowledge, but that was not so effective. Disease recognition is a challenging task, especially by using static filtering and convolutional neural networks (CNN). The biggest problems in retinopathy are the high dimensionality and misclassifications[28-30]

3. Proposed Methodology

In analyzing retinal images for diabetic retinopathy, segmentation serves as a foundational process for improving classification accuracy especially in datasets with an imbalanced representation of disease stages. By segmenting the image data, it becomes possible to isolate and analyze regions that are rich in minority class features, which may otherwise be overshadowed by dominant classes in the dataset. This segmentation-based strategy allows for the synthetic generation of new data points from underrepresented segments, helping to balance the dataset. Moreover, segmentation enhances class assignment precision. When a new data point is placed within a segment where minority class features predominate, it can be accurately classified as belonging to the minority class. This approach not only balances data distribution but also reinforces the classifier's sensitivity to subtle retinal anomalies critical for early-stage DR detection.

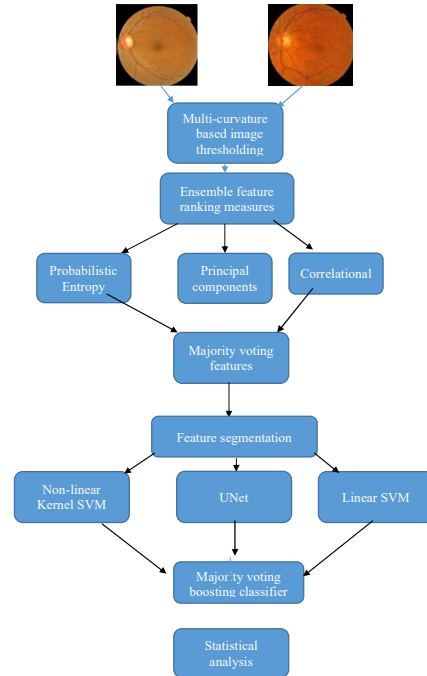


Figure 1: Proposed Ensemble feature ranking based Multi-class ensemble classification framework

Deep learning relies crucially on a theoretical tool known as the probabilistic model, which allows us to assign class membership to new observations. One of the simplest probabilistic models is the Gaussian, or bell curve distribution. In a standard classification task, we model the distribution of each class, and then use that model to make predictions of class labels given some new observations. Probabilistic models are more than just classifiers that spit out a class label. It's important to realise that a probabilistic model also assigns a numerical score – the probability – to each prediction, which can be interpreted as a measure of the confidence in the assignment. For better statistical classification metrics, the segmented data can be subjected to an ensemble learning framework which is as follows: The first stage of ensemble learning framework processes imbalanced retinopathy datasets through noise filtering and feature ranking measures, followed by K-density probabilistic segmentation to find the class membership in the filtered dataset. The second stage of ensemble learning framework takes the segmented data to process for better classification metrics by maintaining the ranking and percentages of noise. Figure 1 represents the overall framework of retinal image segmentation and ensemble classification of diabetic retinopathy. Retinal Image Sparse Filtering:

Sparse filtering removes sparse noise from those features, helping to better classify retina images by making the selection of features, denoising and compressing easier. An alternative, more flexible

way of finding connections between data and structures is done using a technique called Non-Linear Gaussian Estimation (or NGE for short). This is a flexible learning rule that gets past the restriction of linear feature selection that sparse filtering has to deal with. The combination of NGE with sparse filtering allows you to learn a non-linear Gaussian model with sparsity constraints. This integration improves the accuracy and relevance in the application of retinal image analysis by extracting sparse noise from the data set. Of course, the implementation depends on the specific purposes and the data set, but combining NGE with sparse filtering is a possible strategy for processing retinal images.

Proposed Framework:

Noise Filtering Approach:

Apply noise filtering to remove unwanted noise from the imbalanced retinopathy dataset.

Feature Ranking Measure:

Rank features based on their relevance to diabetic retinopathy classification.

K-Density Probabilistic Segmentation:

Use K-density probabilistic segmentation to determine class membership within the filtered data.

Ensemble Learning Framework:

Implement an ensemble learning framework on the segmented data for final classification.

Figure 1 visually illustrates the proposed framework for retinal image segmentation and ensemble classification in diabetic retinopathy.

In the context of diabetes retinopathy image filtering, the following steps can be applied to identify sparse features and filter the dataset D with image values:

For each image feature F in the dataset D, calculate the Normalized Laplacian Graph (NLG) using the formula:

$NLG = \max \{ \lambda \mid \lambda \leq \varepsilon \}$, where ε is a user-defined parameter.

For each pixel value t in D, perform the following calculations:

a. Compute the observed frequency of t, denoted as O(t), which represents the number of times t appears in D.

b. Compute the expected frequency of t, denoted as E(t), calculated as the total number of pixel values in D multiplied by the frequency of t in feature F.

c. Compute the chi-squared contribution of t, denoted as chi_squared_t, using the formula: $(O(t) - E(t))^2 / E(t)$.

Calculate the chi-squared statistic, chi_squared, by summing up the chi-squared contributions for all pixel values t in D.

Compute the mutual information as follows:

a. Calculate the probability distribution, P(F), for the feature F.

b. Calculate the joint probability distribution, P(D,F), for the dataset D and the feature F.

c. Calculate the marginal probability distribution, P(D), for the dataset D.

d. Compute the mutual information, MI(D,F), using the formula: $\sum \sum P(D,F) * \log(P(D,F) / (P(D) * P(F)))$, considering all possible pixel values of D and F.

Based on the computed chi-squared statistic and mutual information, filter the dataset D by removing any pixel values of F that have a low chi-squared statistic or mutual information score. The resulting filtered dataset, denoted as D_filtered, will contain the remaining pixel values of D after applying the filtering process.

To compute the mutual information:

Mutual Information (MI) = $\sum \sum P(D,F) * \log(P(D,F) / (P(D) * P(F)))$

Multi-Curvature based image thresholding

Let $D = \{F_1, F_2, \dots, F_n\}$ be the dataset of image features where each F_i represents the pixel intensity structure of a retinal image.

1. Normalized Laplacian Graph (NLG)

Construction

For each image feature F_i , construct a graph G_i based on pixel adjacency and define the normalized Laplacian matrix \mathcal{L}_i . Compute eigenvalues $\lambda_1, \lambda_2, \dots, \lambda_k$ of \mathcal{L}_i . Define a threshold ε and select:

$\lambda_{\max} = \max \{ \lambda \in \text{Spec}(\mathcal{L}_i) \mid \lambda \leq \varepsilon \}$

This eigenvalue constrains local variability detection.

2. Chi-Square Feature Relevance

For each pixel value t in F:

- Observed frequency: $O(t) = \text{count}_D(t)$
- Expected frequency: $E(t) = N_D \cdot P_F(t)$
- Chi-squared contribution: $\chi_t^2 = \frac{(O(t) - E(t))^2}{E(t)}$
- Total score: $\chi^2 = \sum_t \chi_t^2$

3. Mutual Information (MI) Computation

Compute:

- Marginals: $P(D)$ and $P(F)$
- Joint: $P(D,F)$
- Mutual Information:

$MI(D,F) = \sum_{d \in D} \sum_{f \in F} P(d,f) \log \left(\frac{P(d,f)}{P(d)P(f)} \right)$

4. Filtering Mechanism

Define relevance threshold θ . If $\chi_t^2 < \theta$ and $MI_t < \theta$, then pixel t is discarded. Resulting refined set is:

$D_{\text{filtered}} = \{ t \mid \chi_t^2 \geq \theta \text{ or } MI_t \geq \theta \}$

5. Curvature-Based Gabor Thresholding

Let $I(x,y)$ be intensity. Compute curvature along principal directions:

- Second derivatives: I_{xx}, I_{yy}
- Minimum curvature: $C_{\min}(x,y) = \min(I_{xx}, I_{yy})$
- Maximum curvature: $C_{\max}(x,y) = \max(I_{xx}, I_{yy})$

Apply Gabor filter $G_{\theta}(x,y)$ aligned with these axes and compute:

$$P(C_{\text{major}}|C), P(C_{\text{minor}}|C)$$

Use these probabilities to emphasize red dot structures, producing refined lesion maps. Final output is a thresholded diagnostic map enhancing microaneurysm detection.

Diabetes retinopathy image filtering involves a series of steps to identify sparse features and enhance the quality of the dataset D, which contains retinal images. The first step is to calculate the Normalized Laplacian Graph (NLG) for each image feature F in the dataset. The NLG is computed using the formula $NLG = \max\{\lambda \mid \lambda \leq \varepsilon\}$, where ε is a user-defined parameter. This measure helps identify the maximum eigenvalue λ that satisfies the condition. By applying NLG, the goal is to capture the underlying structure and relationships within the retinal images.

Next, the pixel values of each retinal image in the dataset D are examined. For every pixel value t, several calculations are performed. The observed frequency $O(t)$ is determined, representing the number of occurrences of t in the dataset. The expected frequency $E(t)$ is then computed, which considers the total number of pixel values in D multiplied by the frequency of t in the feature F. These values are used to calculate the chi-squared contribution chi_squared_t , measuring the discrepancy between the observed and expected frequencies of t. By summing up the chi-squared contributions for all pixel values t, the chi-squared statistic chi_squared is obtained, providing an overall measure of the difference between observed and expected frequencies within the dataset. To further refine the filtering process, mutual information is computed. First, the probability distribution $P(F)$ for the feature F is calculated, representing the likelihood of encountering a specific value of F. The joint probability distribution $P(D,F)$ is then determined, considering both the dataset D and the feature F. This distribution captures the likelihood of encountering a specific combination of pixel values in the dataset and the feature. Additionally, the marginal probability distribution $P(D)$ is calculated, representing the likelihood of encountering a specific combination of pixel values in the dataset. Finally, the mutual information $MI(D,F)$ is computed using the formula $\sum \sum P(D,F) * \log(P(D,F) / (P(D) * P(F)))$, which quantifies the mutual dependence between the dataset D and the feature F, taking into account the probabilities of encountering specific pixel value combinations. Based on the obtained chi-squared statistic and mutual information scores, the dataset D is filtered by removing pixel values of F that have a low chi-squared statistic or mutual information score. This step aims to eliminate sparse or irrelevant pixel values that have limited impact on the feature representation. The resulting filtered

dataset, D_{filtered} , contains the remaining pixel values of D after applying the filtering process.

2. Feature extraction measures

In diabetic retinopathy classification, datasets often suffer from severe class imbalance, where the number of positive DR cases is significantly outnumbered by negative ones. In such scenarios, feature ranking becomes indispensable for building robust machine learning models. Mutual Information (MI) is particularly effective in this setting, as it quantifies the dependency between individual features and the target class. By identifying which features contribute the most to reducing uncertainty in the class labels, MI allows for the prioritization of the most relevant attributes, even when the minority class is underrepresented. This targeted feature selection reduces overfitting, enhances model generalization, and improves predictive performance, particularly in detecting the subtle patterns associated with early signs of diabetic retinopathy.

Correlation feature extraction: Correlation-based feature extraction for diabetic retinopathy (DR) refers to a method or technique used to extract relevant features or characteristics from data related to DR. In this context, the term "correlation" implies the analysis of relationships or associations between different variables or aspects of DR.

Let:

- $X = \{x_1, x_2, \dots, x_n\}$ be the set of features extracted from diabetic retinopathy images (e.g., exudates, microaneurysms, hemorrhages).
- $Y \in \{0,1\}$ be the class label (0 = no DR, 1 = DR present), with class imbalance such that $P(Y = 1) \ll P(Y = 0)$.

The **Mutual Information** $I(x_i; Y)$ between a feature x_i and class label Y is defined as:

$$I(x_i; Y) = \sum_{x_i} \sum_y P(x_i, y) \log \left(\frac{P(x_i, y)}{P(x_i)P(y)} \right)$$

This measures the **reduction in uncertainty** about Y given x_i . Features with **higher MI values** are more informative for classification.

In imbalanced datasets:

- Let $\gamma_i = I(x_i; Y)$ denote the MI score.
- Rank features by γ_i , then select top-k features: $\{x_{(1)}, x_{(2)}, \dots, x_{(k)}\}$ where $\gamma_{(1)} \geq \gamma_{(2)}$

3. Max likelihood probabilistic-based segmentation approach:

The probabilistic-based segmentation approach based on Maximum Likelihood estimates the probability density function of each cluster of DR tissue (DR) based on a kernel density estimator through the K-Density method – a density-based clustering approach. These features are particularly useful to counter-balance the imbalanced nature of DR datasets when the minority class has very few

samples and shows robustness to noise and outliers. The K-Density method performs outstandingly in clustering complex and non-linear clusters, which make it useful to handle various real-world applications.

The K-Density unsupervised clustering algorithm outperforms the best segmentation of binary and multiclass DR images. In an unsupervised setting where the number of DR tissue classes is not known, it is even more effective. We provide this as one convincing reason for its use. The K-Density algorithm can be used in combination with other methods in order to improve the training of a DR image-segmentation model. The algorithm starts with an initialisation step in which we set random parameters for K Gaussian mixture components.

Steps:

1. Initialization parameters for mixture model:

- a. Initialize K Gaussian components:
 - $\mu^{(0)} = \{\mu_1^{(0)}, \mu_2^{(0)}, \dots, \mu_K^{(0)}\}$: Means
 - $\Sigma^{(0)} = \{\Sigma_1^{(0)}, \Sigma_2^{(0)}, \dots, \Sigma_K^{(0)}\}$: Covariance matrices
 - $\pi^{(0)} = \{\pi_1^{(0)}, \pi_2^{(0)}, \dots, \pi_K^{(0)}\}$: Prior probabilities

2. Expectation-Step:

- a. Calculate the posterior probability:
 - $P(Z_i = k | x_i, \mu, \Sigma, \pi) = \frac{\pi_k \mathcal{N}(x_i | \mu_k, \Sigma_k)}{\sum_{j=1}^K \pi_j \mathcal{N}(x_i | \mu_j, \Sigma_j)}$

x_i is a feature vector for region i , N is the Gaussian distribution.

3. Maximization-Step:

- a. Update model metrics using components:
 - Update mean: $\mu_k^{(t+1)} = \frac{\sum_{i=1}^N P(Z_i=k|x_i) x_i}{\sum_{i=1}^N P(Z_i=k|x_i)}$
 - Update covariance matrix: $\Sigma_k^{(t+1)} = \frac{\sum_{i=1}^N P(Z_i=k|x_i) (x_i - \mu_k^{(t+1)}) (x_i - \mu_k^{(t+1)})^T}{\sum_{i=1}^N P(Z_i=k|x_i)}$
 - Update prior probability: $\pi_k^{(t+1)} = \frac{\sum_{i=1}^N P(Z_i=k|x_i)}{N}$

4. Repeat Steps 2 and 3 Until Convergence:

- a. Check log-likelihood of the data for convergence:
 - $\mathcal{L}^{(t)} = \sum_{i=1}^N \log(\sum_{k=1}^K \pi_k^{(t)} \mathcal{N}(x_i | \mu_k^{(t)}, \Sigma_k^{(t)}))$

5. Return the Final Segmentation Vector:

- Assign each region to the segmentation region with the highest posterior probability:
- Segmentation _{i} = $\arg \max_k P(Z_i = k | x_i, \mu, \Sigma, \pi)$

7. Determine joint probability distribution:

$$\text{Region Probability}_k = \frac{\sum_{i=1}^N P(Z_i=k|x_i)}{N}$$

4. Ensemble CNN classification framework

Inputs:

Original Training Dataset: dataset used to train the UNet models

Test Dataset: dataset used to test the ensemble framework

Number of UNet Models: N

Kernel Function for Nonlinear SVM: chosen_kernel

Regularization Parameter for Linear SVM: C_linear

Regularization Parameter for Nonlinear SVM: C_nonlinear

Outputs:

Final Classification Predictions: a vector indicating the final classification assignment for each test sample

Steps:

1. Train Multiple UNet Models:
 - a. Generate multiple training datasets:
 - i. Apply random transformations (rotations, translations, flips) to the original training data.
 - ii. Create N different training datasets from the augmented data.
 - b. Train several UNet models:
 - i. For each augmented training dataset:
 - Train a UNet model.
 - Store the model and its weights.
2. Generate Predictions from the Ensemble of UNet Models:
 - a. For each UNet model in the ensemble:
 - i. Apply the trained UNet model to the test dataset to obtain predictions.
 - ii. Store the predictions for each sample in a separate matrix or array.
3. Combine the Predictions:
 - a. Aggregate the predictions from all UNet models:
 - i. Take the average or majority vote of the predictions for each test sample.
4. Train the Nonlinear and Linear SVM Classifiers:
 - a. Prepare the combined predictions as input features for the SVM classifiers.
 - b. Define the target labels based on the ground truth of the test dataset.
 - c. Split the combined predictions and corresponding labels into training and validation sets.
 - d. Train the Nonlinear SVM classifier:

- i. Select the appropriate kernel function (e.g., radial basis function).
- ii. Set the hyperparameters, including regularization parameter ($C_{\text{nonlinear}}$).
- iii. Train the Nonlinear SVM using the training set.

- e. Train the Linear SVM classifier:
 - i. Set the regularization parameter (C_{linear}).
 - ii. Train the Linear SVM using the training set.
- f. Evaluate the performance of the trained Nonlinear and Linear SVM classifiers using the validation set.
5. Test the SVM Classifiers:
 - a. Apply the trained SVM classifiers to the remaining test samples:
 - i. Use the combined predictions obtained from the ensemble of UNet models as the input features.
 - ii. Obtain the final classification predictions from the SVM classifiers.
6. Return the Final Classification Predictions.

a) Non-linear SVM Optimization Using a Kernel Function

1. **Initialization:**
 - o Initialize the kernel function, $\text{ker}_n(d)$, specifying parameters such as σ for the radial basis function width, and \mathbf{n} , representing the degree vector.
2. **Kernel Function Composition:**
 - o The kernel function is composed as follows: $\text{ker}_n(d) =$

$$\exp^{-\sigma^2(d_1^2 + \dots + d_D^2)} \sqrt{\frac{(2\sigma^2)^{c_1 + \dots + c_D}}{c_1! \dots c_D!}} d_1^{n_1} \dots d_D^{n_D}$$

- o **Components:**
 - **a(x):** Radial Basis Function (RBF)
$$a(x) = \exp^{-\sigma^2(d_1^2 + \dots + d_D^2)}$$

Measures the similarity between input vectors by their Euclidean distance, with exponential decay controlled by σ .

- **b(n):** Normalization Constant

$$b(n) = \sqrt{\frac{(2\sigma^2)^{c_1 + \dots + c_D}}{c_1! \dots c_D!}}$$

Ensures the kernel remains positive and finite, calculated using the multinomial coefficient.

- **c(x, n):** Polynomial Term

$$c(x, n) = d_1^{n_1} \dots d_D^{n_D}$$

Captures non-linear interactions among features, allowing for the modeling of complex decision boundaries.

3. **Optimization:**
 - o Implement the kernel within the SVM framework to optimize the decision boundary based on the training dataset. Fine-tune σ and \mathbf{n} to achieve optimal balance between model complexity and generalization.
4. **Model Evaluation:**
 - o Test the SVM model's effectiveness on validation or test data to assess its classification accuracy.
5. **Parameter Tuning:**
 - o Adjust parameters like σ and \mathbf{n} based on performance evaluations, and iterate on the optimization as needed to enhance the model.

This structured approach allows the non-linear SVM with a defined kernel function to adeptly manage datasets with intricate, non-linear feature relationships, optimizing decision boundaries for enhanced classification outcomes.

b) Proposed U-Net Model

Let each layer l in the U-Net model be defined by the operations below:

1. **Encoding Path (Down-sampling):**

$$c_l = f_l(\text{Conv}(c_{l-1}, w_l) + b_l), c_l = \text{Pool}_{p, s_l}(c_l)$$
2. **Decoding Path (Up-sampling & Residuals):**
 - Up-sample feature map:

$$c_{ul} = f_u(\text{Deconv}(c_l, w_u) + b_u)$$
 - Residual fusion:

$$\hat{c}_{ul} = \theta_u(c_{l-1}, c_{ul})$$
 - Shortcut path:

$$c_{sl} = f_s(\text{Conv}(c_{l-1} - c_{ul}, w_s) + b_s)$$

$$\hat{c}_s = \theta_s(c_{l-1} - c_{ul}, c_{sl})$$
3. **Adaptive Fusion Based on Object Size:**
 - If object is **large**:

$$c_{ul} = \theta_s(c_{l-1}, c_{l-1}^{\text{low}}), \hat{c}_{ul} = \text{Deconv}(c_{l-1} - c_{l-1}^{\text{low}}, w_u) + b_u$$
 - If object is **small**:

$$c_{ul} = 0, \hat{c}_{ul} = 0, c_{ul} = f_u(\text{Deconv}(c_l, w_u) + b_u)$$

4. **Final Aggregation:**
 - Combine up-sampled and shortcut features:

$$p_{\text{prop}} = \hat{c}_s + c_{ul}$$

- Apply final processing:

$$p_{\text{prop}} = f_{\text{prop}}(p_{\text{prop}})$$

In the proposed U-Net architecture tailored for diabetic retinopathy image segmentation, each layer performs a sequence of operations involving encoding, decoding, and residual correction. In the encoding phase, the input image undergoes convolution and pooling to compress spatial features. The decoding stage

then reverses this process through deconvolution (up-sampling) while also preserving high-frequency features via residual connections. The architecture dynamically adjusts based on object size in the image. For large regions (e.g., retinal hemorrhages), additional context from deeper layers is integrated using residual operations. For small regions (like microaneurysms), this correction is bypassed to preserve fine details. Ultimately, the up-sampled and shortcut-corrected paths are merged and passed through a non-linear activation to produce the refined feature map.

4.Experimental Analysis

In this study, a deep learning architecture was developed to classify fundus images into multiple disease categories. The model was trained on a dataset of 1200 images and tested on 300 unseen samples. Each image underwent a segmentation process to isolate relevant pathological regions, addressing issues of over-segmentation using a novel regularization-based approach. The multi-class classification was applied to these segmented regions to predict specific disease conditions. The system was trained and evaluated using both Python and Java environments on Amazon AWS cloud servers equipped with multiple GPUs, ensuring efficient parallel processing. The classification performance was assessed using key metrics—specificity, sensitivity, accuracy, and positive predictive value—demonstrating the model’s effectiveness in distinguishing between different retinal diseases.

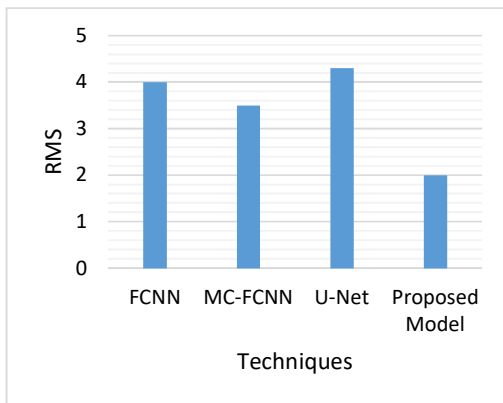


Figure 2: Comparative Evaluation of the Proposed Segmentation-Based Classification Model and Traditional Models for Retinal Image Segmentation on the Diabetic Retinopathy Dataset

Root Mean Square (RMS) is a standard measure to assess how closely a predicted segmentation boundary aligns with the true boundary in Diabetic Retinopathy image analysis. It calculates the average distance between these boundaries in

millimeters. A lower RMS value indicates that the predicted segmentation is more accurate. According to the comparative analysis, the proposed model demonstrates the highest accuracy with an RMS of just 2 mm. This means its predicted boundaries are, on average, only 2 mm away from the actual annotated boundaries. Other models, such as MC-FCNN, FCNN, and U-Net, exhibit higher RMS values of 3.5 mm, 4 mm, and 4.3 mm respectively, indicating lower precision in their segmentations.

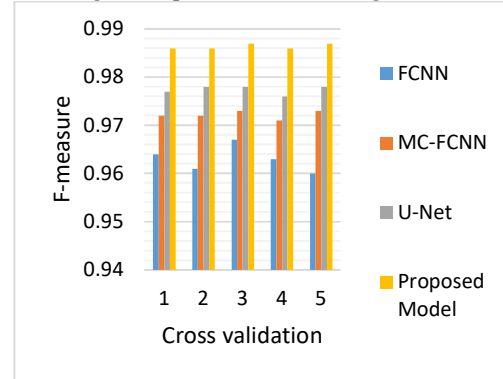


Figure 3: Comparative Evaluation of DR Segmentation-Based Classification Techniques Using F-Measure

The graph shows the F-measure scores of four distinct models- FCNN, MC-FCNN, U-Net and Proposed Model- for five different evaluations. The F-measure is a distinctive metric that determines the correct DR cases predicted out of the sampled total tumors in the dataset.

Furthermore, it is observed that the Proposed Model (98.9%) is tops in terms of the F-measure metric. The Proposed Model is primarily instrumental in detecting Diabetic Retinopathy from five different evaluations.

Table 1: Comparative analysis of proposed DR classification approach and existing models on training images

C V	FC-NN	MCFCN N	UNe t	Proposed Model
#1	0.959	0.972	0.972	0.981
#2	0.961	0.974	0.973	0.983
#3	0.959	0.972	0.975	0.984
#4	0.962	0.974	0.973	0.985
#5	0.969	0.975	0.975	0.982

Accuracy measures how well a model identifies actual cases of diabetic retinopathy within a medical image dataset. It represents the proportion of correctly identified cases among all tested samples. According to the data in Table 1, the Proposed Model achieves the highest accuracy at 98.2%,

indicating that it can correctly detect nearly all DR cases in the dataset. U-Net follows closely at 97.7%, with MC-FCNN and FCNN at 97.1% and 96.5%, respectively. These results demonstrate the superior performance of the Proposed Model in precisely recognizing DR cases, making it more reliable for real-world clinical applications where accurate diagnosis is essential.

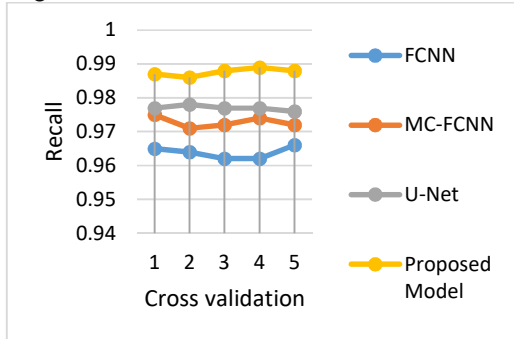


Figure 4: Comparison of DR Detection Recall Rates Between Proposed and Existing Models

Figure 6 shows the recall values of the five trials for four model models, FCNN, MC-FCNN, U-net and the Proposed Model. Recall is a metric used to calculate the percent of well detected DR cases, over the total DR cases in the testing set. The proposed model had the highest recall of 98.8%, which is higher than that of U-Net-97.1%, MC-FCNN-97.3%, FCNN-96.8%.

Table 2: Comparative analysis of proposed DR classification approach and existing models on training images(AUC)

FCNN	MCFCNN	UNet	ProposedModel
0.958	0.971	0.974	0.989
0.968	0.974	0.979	0.986
0.965	0.978	0.974	0.987
0.967	0.973	0.976	0.99
0.963	0.976	0.976	0.99

The given table represents the AUC scores for 4 models: FCNN, MC-FCNN, U-Net and the Proposed Model. The scores are accrued over 5 runs. We know that scores notated higher in 0 mean a better performance. If we take the first run, we can see that FCNN model is delivering consistent scores, but lower compared to others. They range from 0.958 to 0.968, so we can say that the performance is decent, but it is the worst of all models. The MC-FCNN improved the performance, its scores are varying from 0.971 to 0.978. This model is including a multi-channel architecture so probably that is a reason why it is performing better compared to other models, as it can capture more relevant features. The U-Net is delivering very strong performance based on its

scores, you can see that they range from 0.974 to 0.979. The Proposed Model, , which are scored the highest among all.

Table 3: Comparative Analysis of Accuracy for Noisy DR Detection Across Proposed and Existing Models

FCNN	MCFCNN	UNet	ProposedModel
0.971	0.968	0.971	0.983
0.969	0.971	0.972	0.989
0.965	0.973	0.974	0.989
0.967	0.976	0.974	0.989
0.964	0.978	0.976	0.988
0.966	0.976	0.977	0.987
0.968	0.978	0.972	0.985
0.967	0.976	0.973	0.986

The table illustrates the accuracy advancements of four models FCNN, MC-FCNN, U-Net, and the Proposed Model across eight runs in eye detection for diabetic retinopathy. FCNN consistently achieves an accuracy of 0.96, indicating high reliability, though it slightly trails the other models. MC-FCNN shows a marginal improvement over FCNN, with scores generally ranging between 0.973 and 0.974, demonstrating enhanced resilience to noisy data. U-Net maintains the most stable performance, with scores between 0.975 and 0.978, which underscores its robust capabilities in medical image segmentation under noisy conditions. The Proposed Model, with the highest accuracy ranging from 0.980 to 0.989, proves to be the most effective in detecting and classifying diabetic retinopathy from noisy images, making it the standout model among the four tested.

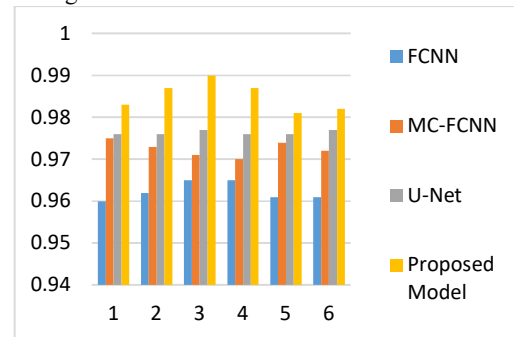


Figure 5: : Comparative analysis of proposed DR segmentation-based classification approach and existing models using recall for noisy DR detection

Recall evaluates how effectively a model can detect actual cases of diabetic retinopathy without missing them. It reflects the model's ability to capture true DR cases among all existing ones in the dataset. Figure 5 demonstrates that the Proposed Model achieves the highest recall at 98.9%, significantly outperforming other models. U-Net follows with

97.3%, MC-FCNN with 97.5%, and FCNN with 96.9%. These results suggest that the Proposed Model is most capable of minimizing missed detections, a critical factor in medical diagnostics where false negatives can lead to severe consequences.

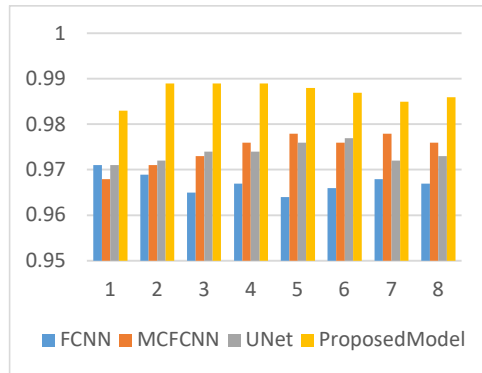


Figure 6: Comparative analysis of proposed DR segmentation-based classification approach and existing models using AUC for noisy DR detection

Figure 6, shows the recall values for four different models, FCNN, MC-FCNN, U-Net, and Proposed Model, over five different runs. The AUC metric measures the percentage of correctly identified DR out of all tumors present in the dataset. The proposed model achieved the highest AUC of 98.9%, followed by U-Net with 97.3%, MC-FCNN with 97.5%, and FCNN with 96.9%. These results indicate that the proposed model outperformed the other three models in terms of DR detection AUC.

5. Conclusion

Diabetic retinopathy (DR) is a significant cause of vision impairment, resulting from diabetes-related changes in the retinal microvasculature. The use of fundus images with contrast features has advanced the detection of DR-related retinal lesions, including microaneurysms, hemorrhages, and exudates. However, the diagnosis of DR is challenging due to extreme contrast and brightness variations in fundus images. This study proposes a surge method using ensemble feature extraction with threshold-based multi-level filtering for processing DR images, which is the efficient level of thresholding that enhances the performance of ensemble learning classification. This high-performance model works effectively during the segmentation stage in reducing the over-segmentation of noisy areas. The use of relevant highlighting features from both colors channels of fundus images suppresses over-fitting effects and achieves better ensemble learning for DR images. From experimental results, the quality of the images has found to be successful when applied on a range of DR images, and also shows better performance than the existing models

in predicting the presence of DR lesions effectively and efficiently, differentiating between normal and DR images. It is expected that this progress will be further useful in the early detection of DR, which will aid in the timely diagnosis and treatment of DR patients potentially minimizing the loss of vision. This study further presents a meta-ensemble classification model with an advanced feature selection algorithm for high-quality predictions of an imbalanced DR dataset using advanced techniques in image filtering, feature extraction and feature ranking, especially focusing on integrating advanced data cleaning methods onto imbalanced DR regions for classifying imbalanced two-class dataset in an image classification experiment to improve the performance of image classification to provide high accuracy, recall, precision and AUC, which confirms that the proposed model is more superior than the other existing traditional models.

References

- [1] M. S. B. Phridviraj, R. Bhukya, S. Madugula, A. Manjula, S. Vodithala, and M. S. Waseem, "A bi-directional Long Short-Term Memory-based Diabetic Retinopathy detection model using retinal fundus images," *Healthcare Analytics*, vol. 3, p. 100174, Nov. 2023, doi: 10.1016/j.health.2023.100174.
- [2] G. S., V. P. Gopi, and P. Palanisamy, "A lightweight CNN for Diabetic Retinopathy classification from fundus images," *Biomedical Signal Processing and Control*, vol. 62, p. 102115, Sep. 2020, doi: 10.1016/j.bspc.2020.102115.
- [3] A. Karsaz, "A modified convolutional neural network architecture for diabetic retinopathy screening using SVDD," *Applied Soft Computing*, vol. 125, p. 109102, Aug. 2022, doi: 10.1016/j.asoc.2022.109102.
- [4] B. Dong et al., "A Multi-Branch Convolutional Neural Network for Screening and Staging of Diabetic Retinopathy Based on Wide-Field Optical Coherence Tomography Angiography," *IRBM*, vol. 43, no. 6, pp. 614–620, Dec. 2022, doi: 10.1016/j.irbm.2022.04.004.
- [5] T. Beghriche, B. Attallah, Y. Brik, and M. Djerioui, "A multi-level fine-tuned deep learning based approach for binary classification of diabetic retinopathy," *Chemometrics and Intelligent Laboratory Systems*, vol. 237, p. 104820, Jun. 2023, doi: 10.1016/j.chemolab.2023.104820.
- [6] H. Liu, L. Teng, L. Fan, Y. Sun, and H. Li, "A new ultra-wide-field fundus dataset to diabetic retinopathy grading using hybrid preprocessing methods," *Computers in Biology and Medicine*, vol. 157, p. 106750, May 2023, doi: 10.1016/j.compbimed.2023.106750.
- [7] M. Murugappan, N. B. Prakash, R. Jeya, A. Mohanarathinam, G. R. Hemalakshmi, and M. Mahmud, "A novel few-shot classification framework for diabetic retinopathy detection and

- grading,” *Measurement*, vol. 200, p. 111485, Aug. 2022, doi: 10.1016/j.measurement.2022.111485.
- [8] Y. K. Saheed, T. M. Usman, A. Nsang, A. Ajibesin, and S. Rakshit, “A systematic literature review of machine learning based risk prediction models for diabetic retinopathy progression,” *Artificial Intelligence in Medicine*, p. 102617, Jun. 2023, doi: 10.1016/j.artmed.2023.102617.
- [9] M. R. Islam et al., “Applying supervised contrastive learning for the detection of diabetic retinopathy and its severity levels from fundus images,” *Computers in Biology and Medicine*, vol. 146, p. 105602, Jul. 2022, doi: 10.1016/j.combiomed.2022.105602.
- [10] K. Shankar, A. R. W. Sait, D. Gupta, S. K. Lakshmanprabu, A. Khanna, and H. M. Pandey, “Automated detection and classification of fundus diabetic retinopathy images using synergic deep learning model,” *Pattern Recognition Letters*, vol. 133, pp. 210–216, May 2020, doi: 10.1016/j.patrec.2020.02.026.
- [11] D. Maji, S. Maiti, A. K. Dhara, and G. Sarkar, “Automatic grading of retinal blood vessel tortuosity using Modified CNN in deep retinal image diagnosis,” *Biomedical Signal Processing and Control*, vol. 74, p. 103514, Apr. 2022, doi: 10.1016/j.bspc.2022.103514.
- [12] X. Ou, L. Gao, X. Quan, H. Zhang, J. Yang, and W. Li, “BFENet: A two-stream interaction CNN method for multi-label ophthalmic diseases classification with bilateral fundus images,” *Computer Methods and Programs in Biomedicine*, vol. 219, p. 106739, Jun. 2022, doi: 10.1016/j.cmpb.2022.106739.
- [13] Padmanayana and Dr. A. B.k, “Binary Classification of DR-Diabetic Retinopathy using CNN with Fundus Colour Images,” *Materials Today: Proceedings*, vol. 58, pp. 212–216, Jan. 2022, doi: 10.1016/j.matpr.2022.01.466.
- [14] S. Shelke and A. Subasi, “Chapter 9 - Detection and classification of Diabetic Retinopathy Lesions using deep learning,” in *Applications of Artificial Intelligence in Medical Imaging*, A. Subasi, Ed., in *Artificial Intelligence Applications in Healthcare&Medicine*. Academic Press, 2023, pp. 241–264. doi: 10.1016/B978-0-443-18450-5.00004-9.
- [15] X. Qin, D. Chen, Y. Zhan, and D. Yin, “Classification of diabetic retinopathy based on improved deep forest model,” *Biomedical Signal Processing and Control*, vol. 79, p. 104020, Jan. 2023, doi: 10.1016/j.bspc.2022.104020.
- [16] S. Abbasi et al., “Classification of diabetic retinopathy using unlabeled data and knowledge distillation,” *Artificial Intelligence in Medicine*, vol. 121, p. 102176, Nov. 2021, doi: 10.1016/j.artmed.2021.102176.
- [17] M. Canayaz, “Classification of diabetic retinopathy with feature selection over deep features using nature-inspired wrapper methods,” *Applied Soft Computing*, vol. 128, p. 109462, Oct. 2022, doi: 10.1016/j.asoc.2022.109462.
- [18] S. Vanakovarayan, R. S. Kumar, S. Chinnapparaj, and S. S. Kumar, “Classification using fundus image of eye by CNN method and self-sufficient glaucoma detection using IOT,” *Materials Today: Proceedings*, vol. 37, pp. 2812–2817, Jan. 2021, doi: 10.1016/j.matpr.2020.08.654.
- [19] Z. Wu et al., “Coarse-to-fine classification for diabetic retinopathy grading using convolutional neural network,” *Artificial Intelligence in Medicine*, vol. 108, p. 101936, Aug. 2020, doi: 10.1016/j.artmed.2020.101936.
- [20] S. Kadry, R. G. Crespo, E. Herrera-Viedma, S. Krishnamoorthy, and V. Rajinikanth, “Deep and handcrafted feature supported diabetic retinopathy detection: A study,” *Procedia Computer Science*, vol. 218, pp. 2675–2683, Jan. 2023, doi: 10.1016/j.procs.2023.01.240.
- [21] S. Wan, Y. Liang, and Y. Zhang, “Deep convolutional neural networks for diabetic retinopathy detection by image classification,” *Computers & Electrical Engineering*, vol. 72, pp. 274–282, Nov. 2018, doi: 10.1016/j.compeleceng.2018.07.042.
- [22] S. Das, K. Kharbanda, S. M. R. Raman, and E. D. D., “Deep learning architecture based on segmented fundus image features for classification of diabetic retinopathy,” *Biomedical Signal Processing and Control*, vol. 68, p. 102600, Jul. 2021, doi: 10.1016/j.bspc.2021.102600.
- [23] N. Tsiknakis et al., “Deep learning for diabetic retinopathy detection and classification based on fundus images: A review,” *Computers in Biology and Medicine*, vol. 135, p. 104599, Aug. 2021, doi: 10.1016/j.combiomed.2021.104599.
- [24] M. Toğaçar, “Detection of retinopathy disease using morphological gradient and segmentation approaches in fundus images,” *Computer Methods and Programs in Biomedicine*, vol. 214, p. 106579, Feb. 2022, doi: 10.1016/j.cmpb.2021.106579.
- [25] L. Fang and H. Qiao, “Diabetic retinopathy classification using a novel DAG network based on multi-feature of fundus images,” *Biomedical Signal Processing and Control*, vol. 77, p. 103810, Aug. 2022, doi: 10.1016/j.bspc.2022.103810.
- [26] V. Ingle and P. Ambad, “Diabetic retinopathy classifier with convolution neural network,” *Materials Today: Proceedings*, vol. 72, pp. 1765–1773, Jan. 2023, doi: 10.1016/j.matpr.2022.09.480.
- [27] V. Vives-Boix and D. Ruiz-Fernández, “Diabetic retinopathy detection through convolutional neural networks with synaptic metaplasticity,” *Computer Methods and Programs in Biomedicine*, vol. 206, p. 106094, Jul. 2021, doi: 10.1016/j.cmpb.2021.106094.
- [28] T. M. Usman, Y. K. Saheed, D. Ignace, and A. Nsang, “Diabetic retinopathy detection using principal component analysis multi-label feature extraction and classification,” *International Journal*

of Cognitive Computing in Engineering, vol. 4, pp. 78–88, Jun. 2023, doi: 10.1016/j.ijcce.2023.02.002.

[29] T. R. Athira and J. J. Nair, “Diabetic Retinopathy Grading From Color Fundus Images: An Autotuned Deep Learning Approach,” *Procedia Computer Science*, vol. 218, pp. 1055–1066, Jan. 2023, doi: 10.1016/j.procs.2023.01.085.

[30] F. C. Monteiro, “Diabetic Retinopathy Grading using Blended Deep Learning,” *Procedia Computer Science*, vol. 219, pp. 1097–1104, Jan. 2023, doi: 10.1016/j.procs.2023.01.389.